Dynamic Localization, Absolute Negative Conductance, and Stimulated, Multiphoton Emission in Sequential Resonant Tunneling Semiconductor Superlattices

B. J. Keay, S. Zeuner, and S. J. Allen, Jr.
Center for Free-Electron Laser Studies, UCSB, Santa Barbara, California 93106

K. D. Maranowski and A. C. Gossard
Materials Department, UCSB, Santa Barbara, California 93106

U. Bhattacharya and M. J. W. Rodwell
Department of Electrical and Computer Engineering, UCSB, Santa Barbara, California 93106
(Received 11 May 1995)

We report the first observation of absolute negative conductance and multiphoton stimulated emission in sequential resonant tunneling semiconductor superlattices driven by intense terahertz electric fields. With increasing terahertz field strength the conductance near zero dc bias decreases towards zero and then becomes negative. This is accompanied by new steps and plateaus that are attributed to multiphoton-assisted resonant tunneling between ground states of neighboring quantum wells accompanied by the stimulated emission of a photon.

PACS numbers: 73.40.Gk, 72.20.Ht, 73.20.Dx

In this Letter we report the observation of dynamic localization and absolute negative conductance (ANC) driven by photon-assisted tunneling in multiquantum well superlattices. Theories predicting dynamic localization and absolute negative conductance in semiconductor superlattices subjected to ac electric fields have existed for 20 years [1], but have not been verified experimentally. These theories are based upon semiclassical models of electron motion in superlattices in the miniband or coherent tunneling regime. An essential feature of these models is Bloch oscillation in the presence of intense high frequency electric fields, high frequency fields sufficient to drive carriers beyond the miniband zone boundary, into a region of k space with negative velocity [1]. However, in this Letter we are concerned with sequential resonant tunneling, distinguished from the former by incoherent tunneling and a loss of phase memory after tunneling into a neighboring well. There has been little discussion about this case, discouraged perhaps by the notion that a ladder of levels, the ground states of superlattice quantum wells in an applied electric field, are all equally populated and therefore offer no net coupling to the photon field [2].

At the outset we wish to distinguish these observations from rectification in asymmetric structures like solar cells, p-n junctions, and Schottky diodes. In the work reported here, we have an essentially symmetric structure and no current flows at zero applied dc bias with or without intense terahertz electric fields. The phenomenon is more closely related to absolute negative conductance in resonant tunneling diodes [3] and in bulk GaAs driven with strong microwave fields at GHz frequencies [4]. Here, in a combined dc and ac electric field the average current can be negative at a positive dc bias because the current on negative swings of the microwave field can be greater than the current on positive swings of the oscillating field. This is a purely classical circuit effect, but analogous to the aforementioned theoretical predictions of absolute negative conductance caused by large k-space excursions in the strongly driven Bloch oscillator [1]. We believe the observations made here are beyond simple rectification in asymmetric structures or the classical absolute negative resistance produced by driving a symmetric device into its differential negative resistance regime with a strong ac field.

Photon-assisted tunneling (PAT) is a well established phenomenon describing quasiparticle tunneling in superconducting electronics in the presence of high frequency radiation [5]. Only recently has it emerged in high frequency transport in semiconductor multiquantum well superlattices [6–9] and nanostructures [10,11]. The recent development of an intersubband laser is thought to rely, under some conditions, on photon-assisted tunneling [12].

The sequential resonant tunneling superlattice used in these experiments is shown in Fig. 1. It consisted of 300 nm of GaAs doped at $n^+ = 2 \times 10^{18}$ cm^{-3}, followed by a 50 nm GaAs spacer layer and ten 15 nm GaAs quantum wells and eleven 5 nm GaAs/$Al_{0.30}Ga_{0.70}As$ barriers and capped by another 50 nm GaAs spacer layer and 300 nm of $n^+ = 2 \times 10^{18}$ cm^{-3} Si doped GaAs. The substrate is semi-insulating and the superlattice and spacer layers were n doped to 3×10^{15} cm^{-3} with Si. These experiments were facilitated by integrating the superlattice into broadband bow-tie antennas. The devices were then glued onto a high resistivity hemispherical silicon lens, and gold wires were bonded to the two gold bows. The experiments were performed over a temperature range of 8–15 K with the sample mounted in a temperature controlled flow-type cryostat with Z-cut quartz windows. Ra-

 0031-9007/95/75(22)/4102(4)$06.00

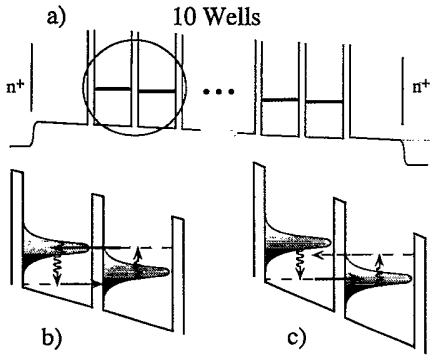

FIG. 1. (a) The superlattice structure under dc bias. (b) Broadened levels in the presence of radiation at low dc bias. For $edE_{dc} < \hbar\omega$, emission channels are inhibited while the absorption channels are enhanced. (c) At higher bias, $edE_{dc} > \hbar\omega$, the absorption channels are inhibited while the emission channels are not. The vertical arrows represent fixed photon energy and the horizontal arrows indicate the resonantly enhanced process (thick arrow) and the impeded process (thin arrow), respectively.

diation was incident on the curved surface of the silicon lens with the polarization parallel to the axis connecting the two gold lobes of the bow-tie.

In Fig. 2 we show the dc current-voltage (I-V) characteristics measured without radiation and with 1.30 THz radiation at three different laser powers. The I-V without laser radiation ($E_{ac} = 0$) shows an Ohmic region characteristic of sequential resonant tunneling followed by sawtooth oscillations associated with electric field domains [13]. At low bias, the current through the sample occurs via ground state to ground state tunneling. As the bias is increased, the current approaches a "critical current," the maximum current that the ground state to ground tunneling will support, and a quantum well breaks off forming a high field domain. The high field domain is characterized by the alignment of the ground state in one well

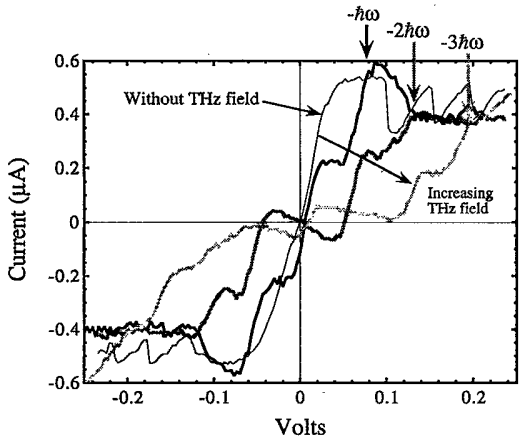

FIG. 2. Current-voltage characteristics measured without radiation and with 1.30 THz (5.38 meV) radiation at three different laser field strengths.

with the excited state in the "downhill" well. As the bias is increased still further one well after another breaks off into the high field domain, indicated by the sawtooth negative differential resistance structure, until the entire sample is encompassed by the high field domain. In this work we are concerned only with the behavior near zero bias, where the transport occurs via ground state to ground state tunneling.

In the presence of a terahertz electric field the conductance at zero bias is first suppressed. That is to say, the terahertz electric field tends to localize the electrons, a manifestation of dynamic localization. However, as the dc bias is increased in one-photon emission channel is brought into resonance with the ground state in the neighboring well and the current increases resulting in the formation of a step in the I-V characteristic. (Note that the voltage where this occurs is approximately $N\hbar\omega/e$, where N is the number of quantum wells. $N = 10$ here.)

At the next higher power shown in Fig. 2, the conductance near the origin actually becomes negative. When this happens the electrons use the absorbed energy from the laser field to tunnel against the applied dc bias. While localization and near zero conductance is predicted, absolute negative conductance is not.

At this level of terahertz excitation, as the dc bias voltage is increased beyond the absolute negative conductance region, the 1-photon emission step is encountered in the I-V characteristic (Fig. 2). The current becomes positive and the electrons are driven down the superlattice accompanied by the stimulated emission of a photon [14]. Remarkably, a 2-photon emission step is also seen at the appropriate voltage. Finally, at the highest power shown in Fig. 2, the 0-photon channel has reappeared, the 1-photon emission step is substantially quenched, the current at the 2-photon step has decreased by a factor of 2, and the formation of the 3-photon emission step is clearly seen at the appropriate bias voltage. The location in voltage of the 1-photon and 2-photon emission steps increases with increasing frequency, as would be expected from multiphoton stimulated emission.

It is clear (Fig. 2) that the transport through various emission channels, as well as the zero bias conductance, is strongly dependent on the laser field strength. In Fig. 3 we show the step height for the 1-, 2-, and 3-photon emission steps and zero bias conductance as a function of terahertz field strength. For the 1-, 2-, and 3-photon processes these steps are defined as the height along the current axis from the base of the step to the upper edge of the step. For each, the step at negative and positive bias has been averaged. The zero bias conductance has been defined as the difference in current measured from the beginning of the Ohmic region at negative bias through the origin to the end of the Ohmic region, measured at positive bias, divided by the voltage difference.

We can project these results on the model of Tien and Gordon in the following way. We assume that the

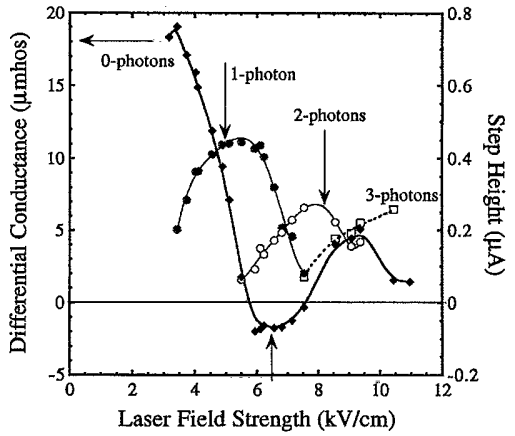

FIG. 3. The step height vs laser field strength for 1-, 2-, and 3-photon assisted tunneling and the zero bias differential conductance, 0-photon process, at 1.30 THz. The three arrows indicate the location of the maximums of J_1^2 and J_2^2, respectively, and the minimum of J_0^2. The lines are to aid the eye.

basic transport mechanism is the sequential tunneling from one quantum well to its neighbor. Following Tien and Gordon [5], we expect that in the presence of a laser field the transition probability to sidebands separated from the ground state by $n\hbar\omega$ is proportional to $J_n^2(\alpha)$, where n corresponds to the net "emission" (negative n) or net "absorption" (positive n), of n photons, and the argument is given by $\alpha = edE_{ac}/\hbar\omega$. Here e is the electron charge, d is the superlattice period, E_{ac} is the THz field strength, and $\hbar\omega$ is the photon energy. In particular, $J_0^2(\alpha)$ describes the suppression of the conductance at zero bias, i.e., dynamic localization, and we expect the conductance to be driven to zero when the argument $edE_{ac}/\hbar\omega$ equals the zero of the $J_0(\alpha)$ Bessel function. Likewise, we expect the new channels at $n\hbar\omega$, that appear as steps at the appropriate bias voltage, to develop in a nonmonotonic way as $J_n^2(\alpha)$.

This is essentially what is observed in Fig. 3. In fact, we can scale the horizontal axis so that the minimum in the zero bias conductance and the maxima in the photon-assisted channels align with the appropriate minimum and maxima of the square of the Bessel functions. The arrows identifying these minimum and maxima are shown in Fig. 3 and can be simultaneously brought into agreement with a single scaling that then defines the field strength inside the superlattice. We conclude that the Tien and Gordon approach is quite adequate.

While the dynamic localization is expected, the absolute negative conductivity does not arise in a straightforward way from this model. As a possible explanation for these observations we propose that the symmetry between the emission and absorption processes is broken by level broadening. This effect is illustrated in Figs. 1(b) and 1(c) where a broadened level in one well is shown, coupled by the laser field to the neighboring well separated by edE_{dc}.

It is important to realize that near the first zero of $J_0^2(\alpha)$ transport will be dominated by the photon-assisted channels. In Fig. 1(b) the applied dc field is less than $\hbar\omega/ed$ and the 1-photon emission channel is impeded, but the absorption channel can proceed and the current will flow against the applied dc bias. As soon as the dc bias exceeds $\hbar\omega/ed$, Fig. 1(c), the picture is reversed and the current will flow in the direction of the applied dc bias.

To model this behavior we assume the broadened levels have state densities $\rho(E)$ given by Gaussians and the occupation is given by a Boltzmann distribution function, $f(E)$. The main assumption being that the carriers are distributed thermally with more at the bottom of the broadened levels than at the top. Following Tien and Gordon we weigh the current through the PAT channels with Bessel functions and model empirically the total ground state to ground state tunneling current according to

$$j \propto \sum_{n=-\infty}^{\infty} J_n^2(\alpha) \int dE\, \rho(E) f(E) \times \{\rho(E - eV_{dc} - n\hbar\omega) - \rho(E + eV_{dc} - n\hbar\omega)\}.$$

We have neglected PAT into excited states, which becomes important at high dc biases and large laser field strengths [9]. The Gaussian density of states is assigned a width of 2 meV, which is almost 2 times the calculated ground state miniband width of 0.55 meV, but is consistent with the broadened width deduced from the I-V characteristic without radiation.

The result of the calculation is shown in Fig. 4. In absence of the THz radiation it can be seen that the Ohmic behavior near zero bias is reproduced by the model. Beyond the Ohmic region (dotted line), however, the model begins to diverge from the experiment. This is due to the fact that the model assumes that the electric field is uniform throughout the superlattices and does not take into account the effect of electric field domains. At the first zero of $J_0^2(\alpha)$ ($\alpha = 2.4$), the 0-photon current has been shut off, the current can only flow through the photon-assisted channels and the current becomes negative near the origin. At the next higher value of laser field strength ($\alpha = 3.3$), a 3-photon emission step is present. Overall, the essential features of the experimental I-V characteristic are reproduced by this simple model. The model does suggest that the phenomenon be explored over a range of temperatures, terahertz frequencies, and level broadening including intrinsic broadening caused by miniband formation.

Negative current flow for small positive dc bias requires level broadening and the tails of the energy levels to extend to within reach of the photon-assisted channel. In this view the absolute negative conductance is an unexpected but reasonable manifestation of dynamic local-

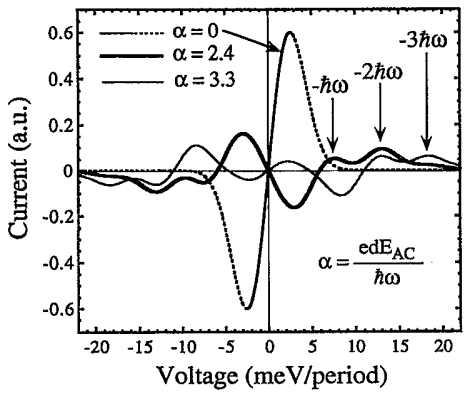

FIG. 4. Current-voltage characteristics produced by the model calculation without radiation and with 1.30 THz radiation at two different laser field strengths.

ization. Furthermore, under dc bias the ladder of quantum well ground states will all be equally occupied and, at first blush, net stimulated absorption or emission of a photon should be absent. By introducing scattering it is apparent that net gain (stimulated emission) can appear on the low frequency side of the Stark ladder splittings and net loss (stimulated absorption) can occur on the high frequency side, relieving the apparent contradiction with Bastard *et al.* [2].

In conclusion, we have observed dynamic localization in a multiquantum well superlattice in the sequential tunneling limit. The dynamic localization is accompanied by negative absolute conductance around zero bias followed by the appearance of photon-assisted channels that correspond to the stimulated emission of as many as 3 THz photons. The essential features of the I-V characteristics are reproduced by a simple empirical model.

We would like to thank the staff at the Center for Free-Electron Laser Studies, J. R. Allen, D. Enyeart, G. Ramian, and D. White. Funding for the Center for Free-Electron Laser Studies is provided by the Office of Naval Research. Additional funding was provided by the Army Research Office, the NSF, and the Air Force Office of Scientific Research.

[1] V. V. Pavlovich and E. M. Epshtein, Sov. Phys. Semicond. **10**, 1196 (1976).

[2] G. Bastard, J. A. Brown, and R. Ferreira, in *Solid State Physics: Semiconductor Heterostructures and Nanostructures,* edited by H. Ehrenreich and D. Turnbull (Academic Press, San Diego, 1994), Vol. 44, p. 325.

[3] J. Sollner *et al.*, in *Physics of Quantum Electron Devices,* edited by Federico Capasso (Springer-Verlag, Berlin, 1990).

[4] Juras Pozhela, *Plasma and Current Instabilities in Semiconductors* (Pergamon, New York, 1981).

[5] P. K. Tien and J. P. Gordon, Phys. Rev. **129**, 647 (1963).

[6] P. S. S. Guimaraes, B. J. Keay, J. P. Kaminski, S. J. Allen, Jr., P. F. Hopkins, A. C. Gossard, L. T. Florez, and J. P. Harbison, Phys. Rev. Lett. **70**, 3792 (1993).

[7] B. J. Keay, P. S. S. Guimaraes, J. P. Kaminski, S. J. Allen, Jr., P. F. Hopkins, A. C. Gossard, L. T. Florez, and J. P. Harbison, Surf. Sci. **305**, 385 (1994).

[8] B. J. Keay, S. J. Allen, Jr., J. P. Kaminski, K. L. Campman, A. C. Gossard, U. Bhattacharya, M. J. W. Rodwell, and J. Galán, in *The Physics of Semiconductors: Proceedings of the 22nd International Conference, Vancouver, Canada, 1994,* edited by D. J. Lockwood (World Scientific, Singapore, 1995), Vol. 2, p. 1055.

[9] B. J. Keay, S. J. Allen, Jr., J. Galán, J. P. Kaminski, K. L. Campman, A. C. Gossard, U. Bhattacharya, and M. J. W. Rodwell, Phys. Rev. Lett. **75**, 4098 (1995).

[10] S. Verghese, R. A. Wyss, Th. Schäpers, A. Förster, M. J. Rooks, and Q. Hu, Phys. Rev. B (to be published).

[11] L. P. Kouwenhoven, S. Jauhar, J. Orenstein, and P. L. McEuen, Phys. Rev. Lett. **73**, 3443 (1994).

[12] J. Faist, F. Capasso, D. L. Sivco, C. Sirtori, A. L. Hutchinson, and A. Y. Cho, Science **264**, 553 (1994).

[13] K. K. Choi, B. F. Levine, R. J. Malik, J. Walker, and C. G. Bethea, Phys. Rev. B **35**, 4172 (1987).

[14] R. F. Kazarinov and R. A. Suris, Sov. Phys. Semicond. **5**, 707 (1971).